A New Experimental Approach for the Evaluation of Domestic Ventilation Systems, Part 1—Description of Experimental Facilities and Their Application to the Quantification of Buoyancy-Driven Airflow in Two-Story Houses

Takao Sawachi, Dr.Eng. **Yoshinori Taniguchi** **Shigeki Ohnishi**

Haruki Ohsawa **Hironaō Setō**

ABSTRACT

A full-scale house model was constructed in an artificial climate chamber, where cylinders were installed for simulating airflow paths, including cracks in the external and internal walls. The flow rate through the cylinders was determined by measuring the pressure difference across them. Ventilation behavior due to internal-external temperature difference, i.e., ventilation induced by buoyancy or stack pressure, was observed without using tracer gas. Parameters such as airtightness of the envelope, airflow resistance through the internal walls, which partly depended upon the operation (open or closed) of doors, and internal-external temperature difference were varied in a series of tests.

After verifying good agreement between calculated values and measurements of the air change rate and pressure difference across the envelope, the air change rate was determined at an inside temperature of 20°C with internal-external temperature differences of 10 K, 20 K, and 30 K, when the reference pressure difference (ΔP_{ref}) is 9.8 Pa and the reciprocal number (n) of the exponential factor of internal-external pressure difference (ΔP) is 2. The air change rate was also calculated at various values of ΔP_{ref} and n to enable prediction of the buoyancy-driven air change rate.

INTRODUCTION

It is well known that indoor air quality has a significant influence on human health. Maintenance of good air quality is a primary concern, especially in residential buildings where occupants stay longer than in other types of buildings. However, current housing trends in North America, Europe, and Japan are toward increased airtightness of the envelopes to achieve higher energy efficiency or to prevent water vapor condensation in the envelope. Accordingly, conventional ventilation techniques not based upon a systematic ventilation scheme are not capable of maintaining good air quality in today's extremely airtight houses.

Current evaluation techniques used in ventilation design for buildings fall into two categories: measurement on site with tracer gas and calculation using a ventilation network model. In domestic ventilation systems, except in the case of central heating or air conditioning where the indoor air is completely mixed, the fresh air supply rates to each room are usually different from each other. Thus, both the tracer measurement technique and the ventilation network model must deal with a multizone situation and identify interzonal airflow rates.

There has been theoretical development and validation by experimental data of tracer gas measurement techniques (Sinden 1978; Afonso et al. 1986; Enai et al. 1990; Okuyama, 1990), and the potential of those techniques has been demonstrated. However, some problems still remain that are related to the effect of measurement error, including uniformity of gas concentration in each single zone and the existence of too many unknown parameters for stability of solutions.

The basic ventilation network model does not require any more validation, but the accuracy of the simulation program should be demonstrated to users so that they do not hesitate to use it for the evaluation of ventilation systems. The benchmark test of different computer codes is also meaningful for testing agreement, but direct comparison with experimental data seems more persuasive. Especially for the prediction of the fresh airflow rate, a relative evaluation among ventilation

Takao Sawachi and Haruki Ohsawa are division heads and **Hironaō Setō** is a senior researcher in the Building Research Institute, Ministry of Construction, Tsukuba, Ibaraki, Japan. **Yoshinori Taniguchi** is a research engineer at the Technical Research & Development Institute, Kumagai Gumi Co. Ltd., Tsukuba, Japan. **Shigeki Ohnishi** is a research engineer with Mitsubishi Electric Corp., Kamakura, Kanagawa, Japan.

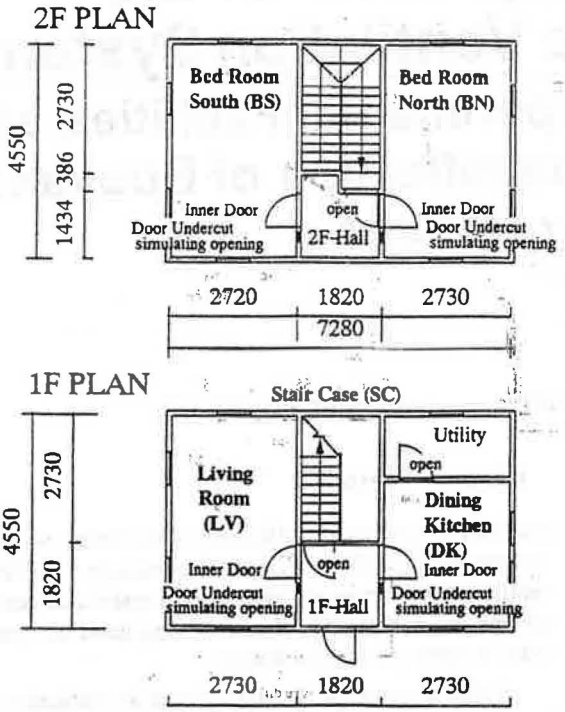

Figure 1 Plan of cylinder house.

systems is not satisfactory, and a comparison between predicted absolute values and standard ventilation requirements is essential.

The apparatus described here can be used for the experimental evaluation of specific ventilation systems as well as being a source of data for the validation of tracer gas measurement techniques and the ventilation network model. As the first application of the experimental equipment, the apparatus was used for observing the airflow induced by buoyancy in a two-story house.

FEATURES OF THE EXPERIMENTAL EQUIPMENT

The equipment is composed of (1) a two-story house with external and internal walls whose airtightness is variable, (2) a large artificial climate chamber enclosing the house, (3) measurement and control systems for pressure difference, temperature, and gas concentration, and (4) a system for measuring ΔP-Q characteristics of components having an airflow path.

Two-Story House

The two-story experimental house is 7.28 m by 4.55 m, with a floor-to-ceiling height of 2.55 m. The room layout is shown in Figure 1. The cubic space of the unit is 176.09 m^3. The inside of the house is divided into ten spaces including an interstory space and an attic. To enable accurate determination of airflow between the inside and outside and between rooms, the house is designed with cracks reduced to the minimum possible extent except for intended openings. To achieve this purpose, each space is separately wrapped with airtight sheets, and highly airtight parts are used for all the doors and windows. To simulate cracks and natural vents, two types of openings are provided in external and internal walls: cylinders 50 mm in inner diameter and 375 mm long for simulating cracks (airtightness control cylinder) and openings of 500 mm x 500 mm or 500 mm x 900 mm for installation of supply-exhaust vents. A total of 163 cylinders are installed in the external walls and 55 in the internal walls (the cylinders in the internal walls are 105 mm long). The latter type of opening is provided at 12 positions in the external walls and 35 positions in the internal floors and ceilings.

TABLE 1
Airtightness of Independent Rooms and Combined Spaces

Rooms or Combined Spaces	Effective Leakage Area ($\times 10^{-4} m^2$)		Effective Leakage Area / Envelope Area ($\times 10^{-4}$)		Effective Leakage Area / Floor Area ($\times 10^{-4}$)		Pressurization or Depressurization
	4 Pa*	9.8 Pa*	4 Pa*	9.8 Pa*	4 Pa*	9.8 Pa*	
LV**	1.25	1.73	0.0202	0.0278	0.101	0.139	Pressurization
DK**	5.75	6.46	0.1209	0.1359	0.661	0.743	Pressurization
UT**	2.77	3.33	0.0978	0.1174	0.743	0.892	Pressurization
BS**	5.22	6.17	0.0843	0.0996	0.421	0.497	Pressurization
BN**	8.07	8.74	0.1303	0.1411	0.650	0.704	Pressurization
1st Floor	5.65	6.53	0.0433	0.0500	0.201	0.232	Pressurization
2nd Floor	6.17	7.41	0.0437	0.0526	0.203	0.244	Pressurization
Whole Rooms as One Space	11.06	13.77	0.0438	0.0545	0.167	0.208	Pressurization
Whole Rooms as One Space	9.89	12.73	0.0391	0.0504	0.149	0.192	Depressurization

* reference pressure ** see room layout of the house (figure 1)

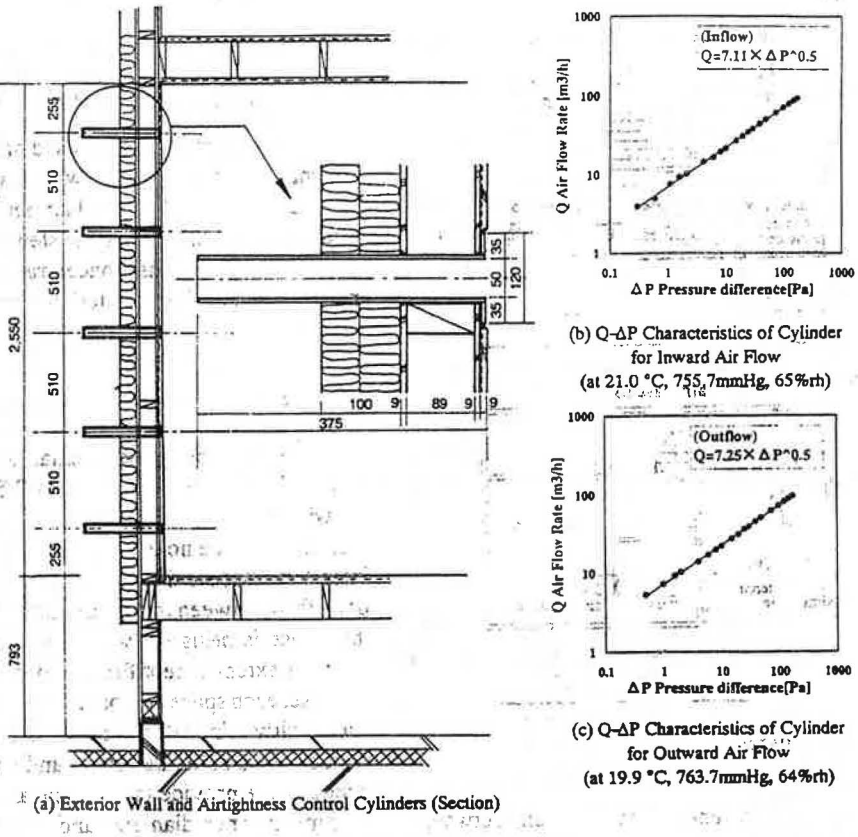

Figure 2 *Vertical layout, detail of installation, and ΔP–Q characteristics of airtightness control cylinder.*

The ΔP-Q characteristics of the airtightness control cylinders are shown in Figure 2. The effective leakage area (reference pressure difference, 9.8 Pa (1 mmAq); discharge coefficient, 1.0) is 15.31 cm^2 for flow into the inside and 15.62 cm^2 for flow to the outside.

The airtightness values of the walls, floors, and ceilings with all the intended openings closed are, as shown in Table 1, very high in all rooms or spaces or combinations of rooms and spaces.

The thermal insulation properties of houses can be adjusted by placing expanded polystyrene panels in the outside of the envelope, such as the external walls and roof. In standard practice, 50-mm-thick expanded polystyrene is installed in two layers. An envelope with such insulation has a thermal transmittance resistance of 4.02°C·m^2/W. The windows are 1360 x 650 mm with sealed double glazing, giving a thermal transmittance resistance of 0.34 °C·m^2/W.

Climate Chamber

The inside dimensions of the climate chamber are 12 m (EW) by 13 m (SN) by 11.05 m high. Free space on the south side, where the house contour is nearest to the chamber wall, is 2 m. The temperature in the chamber is controllable in a range from –10°C to +40°C. The temperature distribution inside the chamber is almost uniform, for example, when set at 30°C and at –10°C for the air-handling units, as shown in Figure 3. The temperatures recorded outside the house as experimental data were determined by T-type thermocouples instead of using the set temperature of the air-handling unit. According to equipment specifications, the airflow velocity should be below 0.3 m/s where the house is close to the chamber wall to prevent airflow in the chamber from driving ventilation in the house. Wind velocity measurements (given in Figure 3) show that this specification is satisfied. Two air-handling units mounted in the west part of the chamber 1.8 m from the house pull return air through the lower grille. Measurements of internal-external pressure difference across the envelope show negligible lowering of pressure in the west of the house; hence, the ventilation driving force in the house due to air suction by the air-handling units has been proved to be negligible.

By using a great air change rate for the chamber, ventilation experiments using tracer gas can be performed as if the house were constructed outdoors. At the maximum, there is ventilation at a rate of 448 m^3/min and an air change rate of 14.5 1/h. When the assumed air change rate is relatively large, e.g., 3 (1/h) for a house of about 260 m^3 including the interstory and attic spaces, deviation from the true ventilation rate

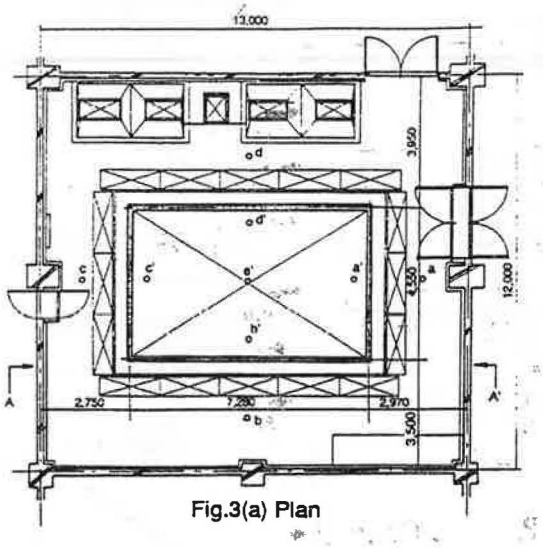

Fig.3(a) Plan

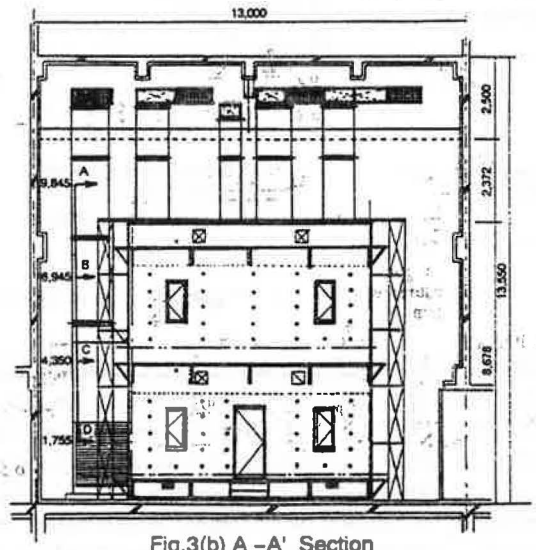

Fig.3(b) A –A' Section

Temperature Distribution in Artificial Climatic Chamber When Ventilated at a Maximum and Target Temp. is 30 deg.C

temperature deg.C		vertical position in Fig.3(b) A	B	C	D
horizontal position in Fig.3(a)	a	–	30.0	29.8	29.6
	b	–	29.5	29.5	29.5
	c	–	29.8	29.5	29.5
	d	–	29.6	29.6	29.6
	a'	–	–	–	–
	b'	–	–	–	–
	c'	–	–	–	–
	d'	–	–	–	–
	e'	29.5	–	–	–

Temperature Distribution in Artificial Climatic Chamber When not Ventilated and Target Temp. is -10 deg.C

temperature deg.C		vertical position in Fig.3(b) A	B	C	D
horizontal position in Fig.3(a)	a	–	-9.3	-8.0	-8.2
	b	–	-8.6	-8.9	-8.7
	c	–	-9.4	-9.1	-8.6
	d	–	-9.2	-8.6	-8.2
	a'	–	–	–	–
	b'	–	–	–	–
	c'	–	–	–	–
	d'	–	–	–	–
	e'	-9.8	–	–	–

Mean Velocity Distribution in Artificial Climatic Chamber When Ventilated at a Maximum

mean velocity (m/s)		vertical position in Fig.3(b) A	B	C	D
horizontal position in Fig.3(a)	a	–	0.22	0.29	0.17
	b	–	0.27	0.11	0.15
	c	–	0.18	0.27	0.33
	d	–	0.22	0.25	0.28
	a'	0.10	–	–	–
	b'	0.27	–	–	–
	c'	0.21	–	–	–
	d'	0.27	–	–	–
	e'	0.18	–	–	–

Figure 3 *Dimension of artificial climatic chamber and temperature and velocity distribution.*

as measured by the tracer gas decay method is estimated to be within 4%.

Measurement and Control Systems

The pressure difference was measured by gauges installed at 14 points (P1 through P14), shown in Figure 4. In addition, the pressure difference between rooms, used as reference data, was measured at four points (P15 through 18). Scans of these were performed at ten-second intervals to record the average for one minute. The dry-bulb temperature was recorded at one-minute intervals at eight points in the climate chamber and 27 points inside the house, while surface temperatures of the walls, floors, ceilings, and glass were recorded at 165 points. In eight spaces (excluding the attic and interstory spaces), 13 electric heaters (600 W or 1200 W) were provided. The temperature in each room was regulated by PID (proportional plus integral plus derivative) control by a microcomputer. Tracer gas could be released at eight points in the house, with sampling at eight points inside the house and four points in the climatic chamber.

Measurement System for ΔP-Q Characteristics

The air leakage characteristics of these components, such as airtightness control cylinders, were measured by a system composed of airtight iron boxes (2000 mm x 2000 mm x 2300 mm) that could fix the components and determine the pressure difference across the cylinders, fan (0.75 W), and duct (200 mm

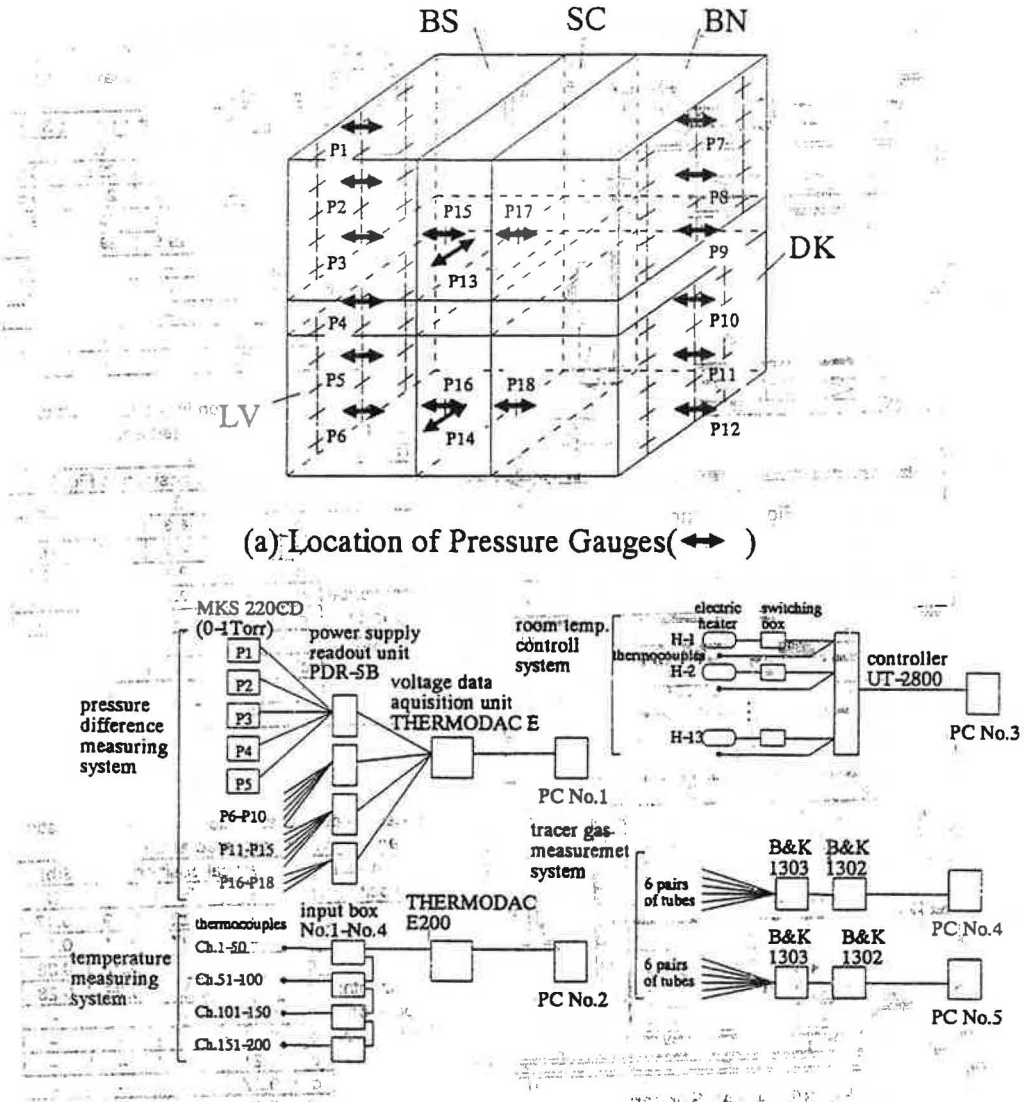

Figure 4 *Measurement and control system.*

in diameter) with a microwave flowmeter or piping with orifices for measuring the microflow rate.

OBSERVATION RESULTS OF BUOYANCY-DRIVEN AIRFLOW IN THE TWO-STORY HOUSE

The main reasons for making the building envelope airtight are to limit the increase of heating load due to air leakage and to prevent water vapor condensation caused by humidity penetrating through the walls. When an airtight envelope is to be constructed, suitable ventilation design is required to compensate for decrease of natural ventilation. The most essential information for the ventilation design is the level of airtightness at which satisfactory airflow cannot be ensured by natural ventilation alone.

Previous studies (ASHRAE 1989; Sherman and Grimsrud 1980; Shaw 1987) have demonstrated (1) that the effects of temperature difference and wind pressure, which are primary elements for inducing ventilation, are not reduced by interaction between them when the overall house is considered and (2) that the effect of temperature difference is more significant than that of wind pressure, especially in densely built-up areas, although it depends upon climatic conditions. For example, when a comparison is made between the effect of 3 m/s wind and 10 K temperature difference by using the ASHRAE prediction method (ASHRAE 1989) of natural

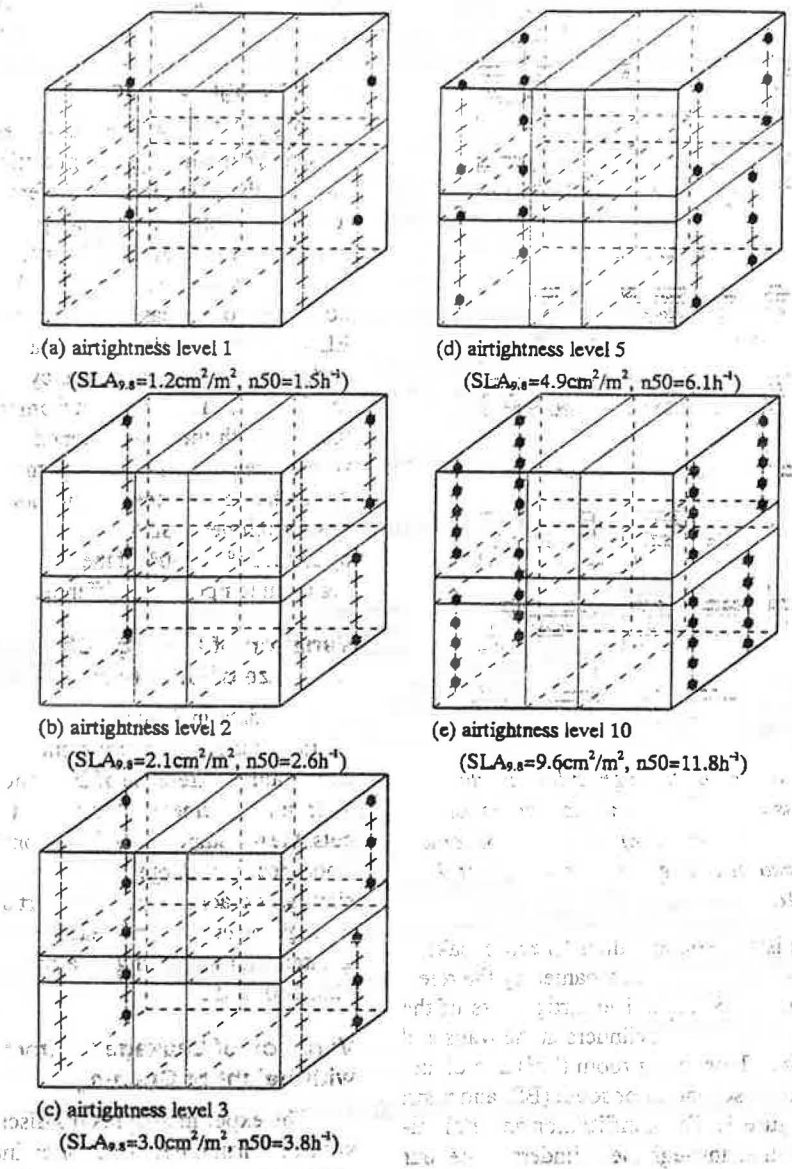

Figure 5 Location of open cylinders (black spots) for each airtightness condition.

ventilation, the increase in ventilation rate by the addition of wind effect is estimated to be 20% while that by the addition of buoyancy effect is estimated to be 83% for a typical suburban shielding condition.

The experimental results presented here show the influence on the natural ventilation rate of envelope airtightness and internal-external temperature difference. The test facilities employed were intended for observing airflow in the house built inside the chamber, not for monitoring the effect of wind on natural ventilation, which requires special pressurization and depressurization devices for the envelope. Because this study is the first step of the research project, we have not tried to provide such devices. Accordingly, the data given in this paper refer to airflows across the envelope and inside the house driven by buoyancy alone. Reference to these data will give a conservative estimate of the natural ventilation rate.

EXPERIMENTAL CONDITIONS

The essential parameters considered when determining the experimental conditions were internal-external temperature difference, airtightness of the envelope and status of the internal doors (open or closed), and leakage area of the undercuts. Three temperature differences were selected, 10 K, 20 K, and 30 K, and five effective leakage areas of the envelope per unit floor area, 1.2, 2.1, 3.0, 4.9, and 9.6 cm^2/m^2 (reference pressure difference is 9.8 Pa [1 mmAq]). The effective leakage

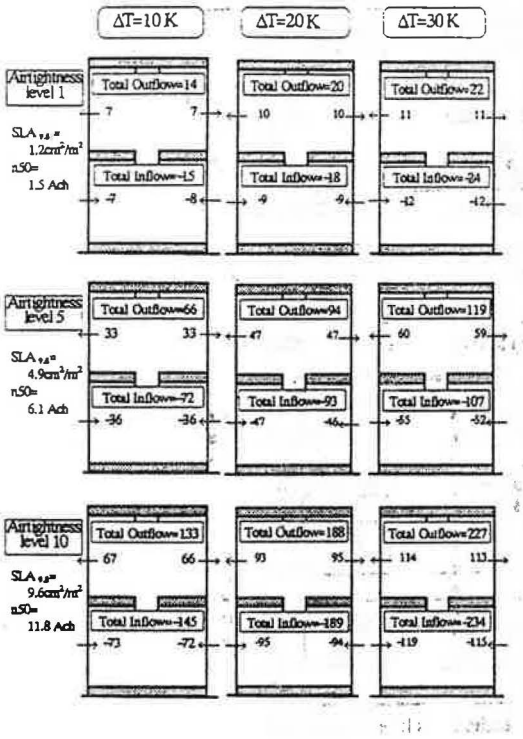

Figure 6 *Airflow rate (m^3/h) through cylinders due to stack pressure with all interior doors open (single space condition). $SLA_{9.8}$: Specific leakage area at the reference pressure of 9.8 Pa (1mmAa).*

area per unit floor area is sometimes called "specific leakage area," which is designated as SLA accompanied by the reference pressure ΔP (Pa), i.e., $SLA_{\Delta P}$. The airtightness of the house was adjusted by opening the cylinders in the walls and internal doors of the first floor living room (LV) and dining kitchen (DK) as well as the second floor south (BS) and north (BN) bedrooms (see Figure 5). Thus, infiltration and exfiltration airflows were generated through the cylinders in the four rooms, except for unintended cracks. With regard to door status and leakage area of the undercuts, five cases were selected: all internal doors opened and doors closed with undercuts of 17, 74, 136, and 223 cm^2 in effective leakage area at a reference pressure difference of 9.8 Pa (1 mmAq).

EXPERIMENTAL RESULTS

Air Leakage Characteristics with Internal Doors Open

Figure 6 shows the measured airflow rates at three temperature differences and three levels of envelope airtightness. Positive values represent outflow from the house, and negative values represent the inflow. Driven by the buoyancy due to the air density difference between both sides of the house, outside air flows into the two rooms on the first floor (LV and DK), then passes through the first floor hall, staircase, and second floor hall, enters the two second floor rooms (BS and BN), and escapes to the climate chamber.

Air Leakage Characteristics with Doors Closed

Figure 7 shows results of tests with the internal doors closed, where the significant airflow paths are door undercuts alone, at three temperature differences and five levels of envelope airtightness. A circular opening 160 mm in diameter was made at the side of each door to simulate the door undercut. The effective leakage area of each circular opening is 136 cm^2, obtained from measurements of ΔP-Q characteristics. This ELA value was selected so that it approximates an ordinary undercut. Induced by buoyancy, the outside air flows in from the first floor and flows out from the second floor, as found in the case with the doors opened. What should be noted is that with decreasing envelope tightness, the difference in leakage due to the status of the internal doors is more remarkable. With low airtightness ($SLA_{9.8}$ = 9.6 cm^2/m^2), the leakage increases by about 35% to 50% if the internal doors are opened, depending upon temperature difference.

Variation of Leakage Characteristics with Size of Undercut

The data in Figure 8(a) indicate the variation of leakage characteristics with undercut size at an internal-external temperature difference of 20 K and airtightness at 4.9 cm^2/m^2. With small-diameter openings (50 mm) for simulating undercuts, the resistance of airflow from the first floor to the second floor becomes larger, resulting in infiltration through the simulated cracks in the lower part of the rooms and exfiltration through the upper part in each floor. The leakage rate becomes greater with increasing size of the opening, from 50 mm to 120, 160, and 200 mm.

Variation of Leakage Characteristics with Height of Opening

The experimental results discussed above were obtained with the airtightness control cylinders opened (one or more cylinders per room) in the two floors and placed symmetrically in the middle of the floor-to-ceiling height. In another arrangement, a single open cylinder was placed in each room in both floors, changing its height to five different levels to observe the variation of leakage characteristics (Figure 9). When the cylinder height in the first and second floors is the same, 3.99 m (see (a), (b), and (d) in Figure 9), the leakage rate is almost the same, whereas the variation ratio is $(1.96/3.99)^{0.5}$ for a smaller difference in height, 1.96 m, and $(6.03/3.99)^{0.5}$ for a larger difference in height, 6.03 m.

DISCUSSION OF EXPERIMENTAL RESULTS

With the same airtightness of the envelope ($SLA_{9.8}$ = 4.9 cm^2/m^2, $n50 = 6.1\ h^{-1}$), as indicated in Figure 8, the buoyancy-driven ventilation rate changes with airflow characteristics of the internal walls from 62 m^3/h to 94 m^3/h, i.e., the increase

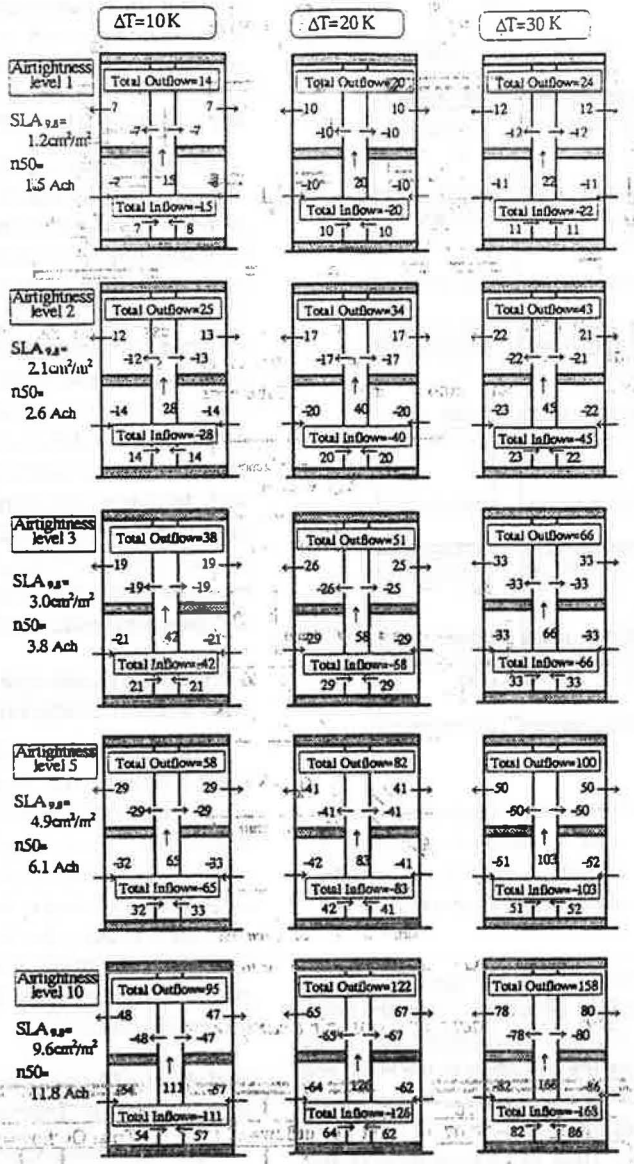

Figure 7 Airflow rate (m^3/h) through cylinders due to stack pressure with four interior doors closed and with undercut simulating cylinders of 160 mm diameter open (multiple space condition). $SLA_{9.8}$: Specific leakage area at the reference pressure of 9.8Pa (1mmAq).

ratio attaining 1.5 at the maximum. When the airtightness of the internal walls is higher than the envelope, as shown in Figure 8(a), outside air flows in through a lower part of the room and escapes through an upper part.

Figure 8(b) shows a comparison—based on the data given in Figures 6 and 7 of the buoyancy-driven airflow rates—between the case with the doors open and the case with the doors closed and undercuts serving as the main flow path. To about 3 cm^2/m^2 of $SLA_{9.8}$, at temperature differences of 10 K to 30 K, the difference due to the status of the door (opened or closed) is not remarkable. However, when the tightness of the envelope is less, the influence due to the status of the door becomes more significant. For districts with a relatively mild climate where the internal-external temperature difference is around 10 K in winter, it is not unrealistic to set $SLA_{9.8}$ to 10. In such a case, the ventilation rate due to buoyancy with the doors open can be estimated to be about 35% greater than with the doors closed. In other words, if the expected buoyancy-induced ventilation rate is based on the case with the doors open, the rate with the doors closed is only about three-fourths of the expected rate.

In measurements of natural ventilation by the tracer gas decay method, the doors are opened and the air is agitated with a fan to achieve a uniform gas concentration in the whole

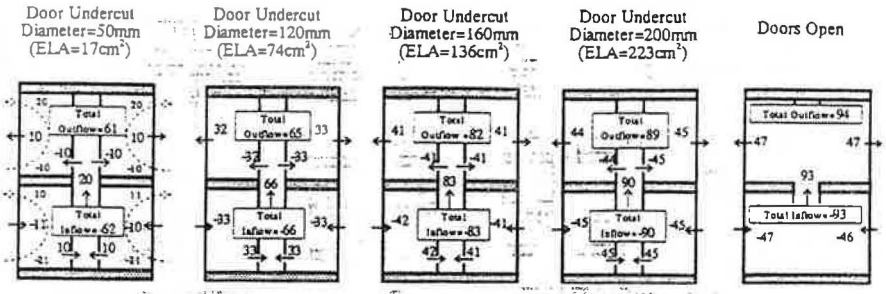

(a) Air Flow Rate (m^3/h) through Cylinders due to Stack Pressure, with Partitions of Different Flow Resistance, with the Envelope Airtightness of $4.9cm^2/m^2$ ($SLA_{9.8}$), under 20 K Indoor-Outdoor Temperature Difference

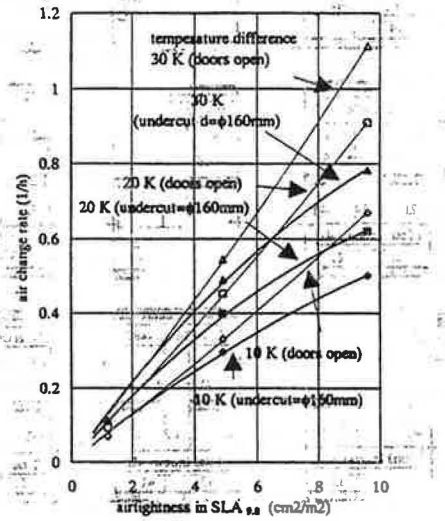

(b) Air Change Rate Difference due to Partition Status

Figure 8 *Effect of partition airflow characteristics on air change rate.*

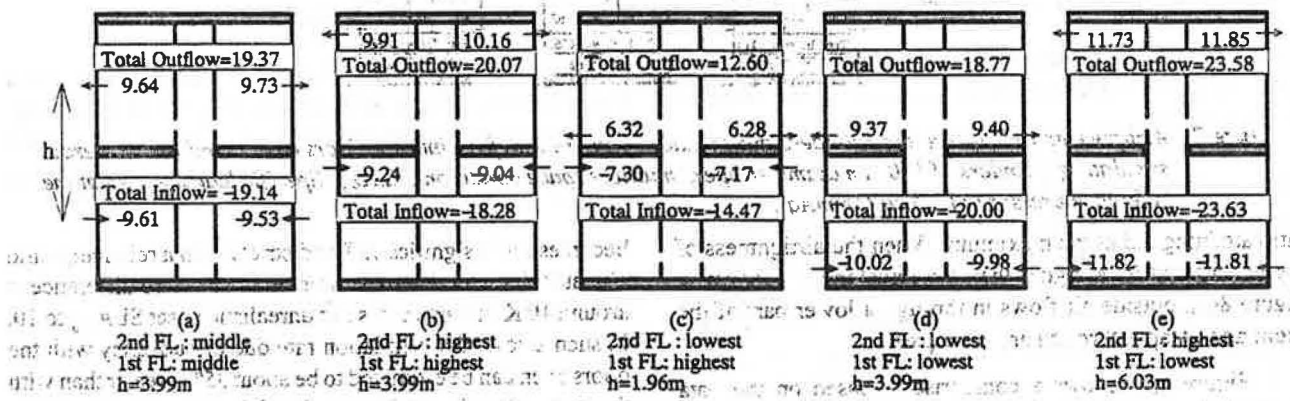

Figure 9 *Airflow rate (m^3/h) through cylinders of the same number at different vertical positions. $SLA_{9.8}$: 1.2 cm^2/m^2; temperature difference: 20 K.*

building. It should be noted that by this practice, the ventilation rate of the house is overestimated because occupants usually close the doors. To make a safe estimation of the natural ventilation rate, other tracer gas techniques, such as the constant concentration method, should be applied with the doors closed. Though the actual status of doors may depend

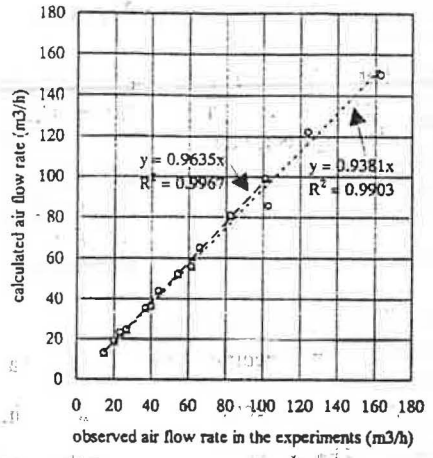

(a) Comparison between Air Flow Rates Calculated and Observed in the Experiments

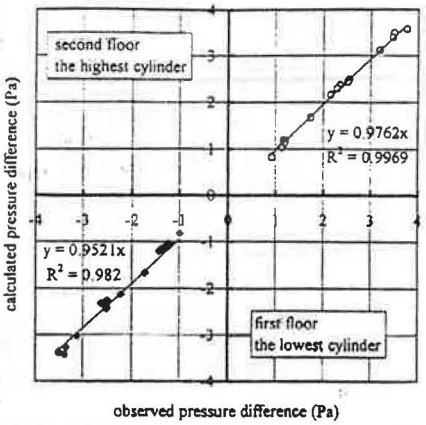

(b) Comaprison of Pressure Difference between Calculation and Observation in the Experiments

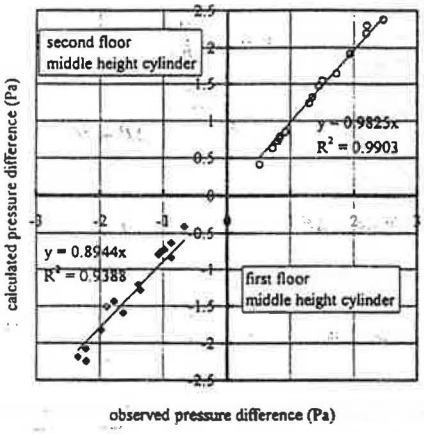

(c) Comaprison of Pressure Difference at the middle height between Calculation and Observation in the Experiments

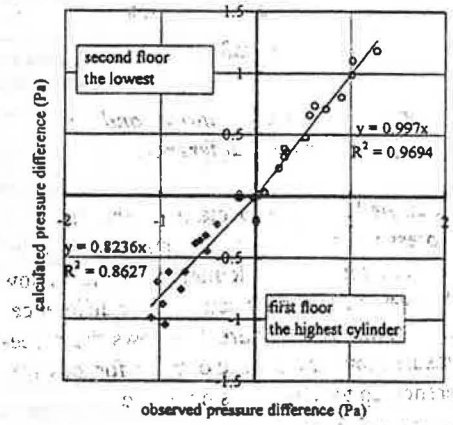

(d) Comaprison of Pressure Difference between Calculation and Observation in the Experiments

Figure 10 Comparisons of airflow rate and pressure difference between experiment and calculation

upon family composition, the discussion here assumes the doors are closed and have open undercuts of 136 cm^2 of effective leakage area.

Comparison of the measured results shown in Figure 7 and calculated values verifies the reliability of both. The calculation was conducted as follows. Letting the internal-external pressure difference at the first floor level $-\Delta P$ ($\Delta P > 0$) be an unknown, the outflow and inflow rates are expressed as a function of ΔP using the crack flow equation (ΔP-Q characteristics) of the cylinders. Referring to the pressure difference at the height of the cylinders, ΔP is determined by iteration so that the sum of the outflow and inflow rates becomes zero. The pressure loss across the undercuts can be given as a function of ΔP by inputting the airflow rate through each room on the first floor, which is expressed as a function of ΔP, in the crack flow equation for the undercuts.

Figure 10(a) shows a comparison of measured data and calculated values for airflow rate. The measured data, in general, are slightly greater than the calculated values. For a ventilation rate of 100 m^3/h or less, they agree fairly well, differences being within 4%. However, in the range of greater flow rates, the difference becomes larger, that is, about 6% as a whole.

Figure 10(b), 10(c), and 10(d) compare measurements and calculations for the pressure difference across the envelope. Comparing both values for the internal-external pressure difference across the lowest cylinders in the first floor walls shows that the calculated values are about 5% smaller than the measurements (third quadrant of Figure 10(b)). For the internal-external pressure difference across the highest cylinders, too, the calculated values are about 2% smaller than the measurements (first quadrant of Figure 10 (b)). The plots for the pressure differences across the highest cylinders in the first floor and the lowest cylinders in the second floor (Figure 10(d)) show that the calculated results for the first floor are 18% smaller than the observed values. The measurements are

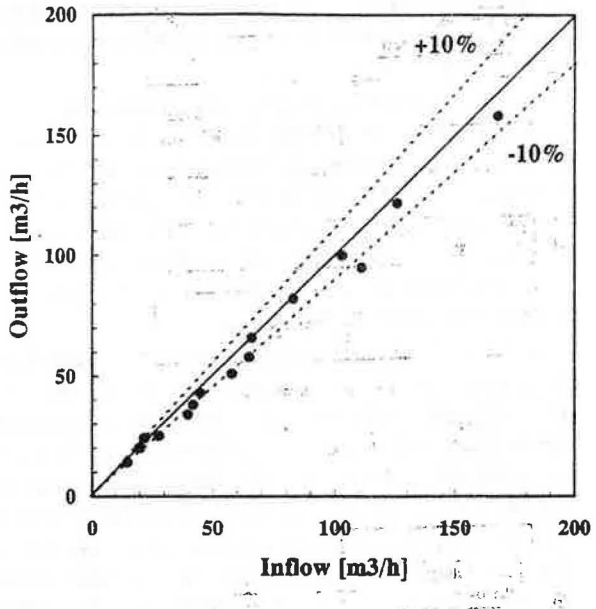

***Figure 11** Comparison between inflow and outflow caused by temperature difference.*

greater than the calculated values, especially for the first floor internal-external pressure difference, reflecting the differences between measurements and calculation for the airflow rates induced by buoyancy. The main cause of the differences seems to be measurement error. Figure 11 shows the agreement between measured total inflow and outflow for the overall house. A difference up to ±10% was observed.

Cracks are provided at five different heights on each floor in the cylinder house. What difference is produced in the airflow rate if cracks are distributed uniformly in the walls and if cracks are present not only in the walls but also in the ceilings and floors? To study these problems, calculations were performed. Equation 1a is the crack flow equation for when the inside of the envelope is negatively pressurized and Equation 1b for when the inside of the envelope is positively pressurized.

$$Q = k_1 \Delta P^{1/n_1} \quad (\gamma_1 \text{ as specific gravity of air}) \tag{1a}$$

$$Q = k_2 \cdot \Delta P^{1/n_2} \quad (\gamma_2 \text{ as specific gravity of air}) \tag{1b}$$

Equation 1c is the ΔP-Q characteristics of an undercut opening of 160 mm diameter.

$$Q = K \cdot \Delta P^{1/m} \quad (\gamma_u \text{ as specific gravity of air}) \tag{1c}$$

Let S_c, S_w, and S_f be the distribution ratios of cracks in the second floor ceilings, the external walls of each story, and the floors of the first floor, respectively. Thus,

$$S_c + 2S_w + S_f = 1 \tag{2}$$

Let ΔP be the internal-external pressure difference at the surface level of the first floor. The inflow rate through the floor, Q_f, is given by

$$Q_f = -S_f \cdot k_1 \cdot \left(\frac{\gamma_1}{\gamma_o}\Delta P\right)^{1/n_1} \cdot \frac{\gamma_o}{\gamma_i} \tag{3}$$

where

γ_o = specific gravity of outdoor air,

γ_i = specific gravity of indoor air.

The inflow rate through the first floor walls, Q_{w1}, is expressed by

$$Q_{w1} = -S_w \cdot \frac{k_1}{h}\left(\frac{\gamma_1}{\gamma_o}\right)^{1/n_1} \frac{\gamma_o}{\gamma_i} \cdot \frac{1}{\gamma_o - \gamma_i} \cdot \frac{n_1}{n_1 + 1} \cdot \left[\Delta P^{\frac{n_1+1}{n_1}} - \{\Delta P - (\gamma_o - \gamma_i)h\}^{\frac{n_1+1}{n_1}}\right] \tag{4a}$$

when $\Delta P - (\gamma_o - \gamma_i)h \geq 0$ and by

$$Q_{w1} = -S_w \cdot \frac{k_1}{h}\left(\frac{\gamma_1}{\gamma_o}\right)^{1/n_1}\gamma_o \frac{1}{\gamma_i} \cdot \frac{1}{\gamma_o - \gamma_i} \cdot \frac{n_1}{n_1 + 1} \cdot \Delta P^{\frac{n_1+1}{n_1}} + S_w \cdot \frac{k_2}{h}\left(\frac{\gamma_2}{\gamma_o}\right)^{1/n_2} \frac{1}{\gamma_o - \gamma_i} \cdot \frac{n_2}{n_2 + 1} \cdot \{(\gamma_o - \gamma_i)h - \Delta P\}^{\frac{n_1+1}{n_1}} \tag{4b}$$

when $\Delta P - (\gamma_o - \gamma_i)h < 0$

where

h = floor-to-ceiling height.

The outflow rate through the second floor walls is obtained by

$$Q_{w2} = S_w \cdot \frac{k_2}{h}\left(\frac{\gamma_2}{\gamma_i}\right)^{1/n_2} \frac{1}{\gamma_o - \gamma_i} \cdot \frac{n_2}{n_2 + 1} \cdot \left[\left\{(\gamma_o - \gamma_i)(H + h) - \Delta P - 2\frac{\gamma_i}{\gamma_u}\left(\frac{Q_f + Q_{w1}}{K}\right)^m\right\}^{\frac{n_2+1}{n_2}} - \left\{(\gamma_o - \gamma_i)H - \Delta P - 2\frac{\gamma_i}{\gamma_u}\left(\frac{Q_f + Q_{w1}}{K}\right)^m\right\}^{\frac{n_2+1}{n_2}}\right] \tag{5a}$$

when $\Delta P \leq (\gamma_o - \gamma_i)H + 2\frac{\gamma_i}{\gamma_u}\left(\frac{Q_f + Q_{w1}}{K}\right)^m \leq 0$

$$Q_{w2} = S_w \cdot \frac{k_2}{h}\left(\frac{\gamma_2}{\gamma_i}\right)^{1/n_2} \frac{1}{\gamma_o - \gamma_i} \cdot \frac{n_2}{n_2+1} \cdot \left\{(\gamma_o - \gamma_i)(H+h) - \Delta P - 2\frac{\gamma_i}{\gamma_u}\left(\frac{Q_f + Q_{w1}}{K}\right)^m\right\}^{\frac{n_2+1}{n_2}} - S_w \cdot \frac{k_1}{h}\left(\frac{\gamma_1}{\gamma_i}\right)^{1/n_1} \frac{1}{\gamma_o - \gamma_i} \cdot \frac{n_1}{n_1+1} \cdot \left(\frac{\gamma_o}{\gamma_i}\right) \cdot \left\{\Delta P - (\gamma_o - \gamma_i)H + 2\frac{\gamma_i}{\gamma_u}\left(\frac{Q_f + Q_{w1}}{K}\right)^m\right\}^{\frac{n_1+1}{n_1}} \quad (5b)$$

when $\Delta P - (\gamma_o - \gamma_i)H + 2\frac{\gamma_i}{\gamma_u}\left(\frac{Q_f + Q_{w1}}{K}\right)^m > 0$

where

H = floor-to-floor height.

The outflow rate through the second floor ceilings, Q_c, is expressed by

$$Q_c = S_c \cdot k_2 \cdot \left\{(\gamma_o - \gamma_i)(H+h) - \Delta P - 2\frac{\gamma_i}{\gamma_u}\left(\frac{Q_f + Q_{w1}}{K}\right)^m\right\}^{1/n_2} \cdot \left(\frac{\gamma_2}{\gamma_i}\right)^{1/n_2} \quad (6)$$

The overall airflow is obtained by calculating ΔP by iteration until the sum $Q_f + Q_{w1} + Q_{w2} + Q_c$ becomes 0, then inputting the obtained ΔP in Equations 3 through 6.

Figure 12 plots the calculated values for the case where cracks have the same overall leakage area as that of the cylinders and are uniformly distributed in the walls ($S_w = 0.5$, $S_c = S_f = 0$) and the case where cracks are uniformly distributed in the ceilings, floors, and walls proportionally to the area of each element ($S_c = S_f = 0.177$, $S_w = 0.323$) against the values calculated for simulation as discussed above. When the cracks are supposed to be uniformly distributed in the walls, there is almost no significant difference from the simulation with the cylinders. In contrast, for the case where cracks are distributed in the ceilings and floors too, the airflow rate is 10% larger in every calculation condition.

In designing for the airtightness of houses, it is essential to know at what level of airtightness sufficient airflow is not ensured by natural ventilation alone. As mentioned before, previous studies suggest it may be unnecessary to consider adverse interference between buoyancy and wind, which are the driving forces for natural ventilation. Therefore, if natural ventilation due to buoyancy alone is taken into account, excluding the wind effect, the resultant prediction of airflow rate is conservative. In the event the air inflow is excessive due to wind, which may degrade the thermal environment inside the house, a solution is the addition of vents, which automatically regulate the airflow rate to avoid excessive ventilation (IEA 1996).

The floor-to-floor height of the cylinder house is 3.99 m, which is higher than ordinary residences. So calculations similar to the one above were conducted assuming a floor-to-floor height, H, of 2.99 m and an inside temperature of 20°C with the internal-external temperature difference produced by varying the outside temperature. Such computational results will contribute to generalizing the airflow prediction for common two-story houses.

Figure 13a illustrates the relationship between the buoyancy-induced ventilation rate (air change rate) and the tightness of the envelope with different internal-external temperature differences. The airflow rates in the figure are obtained when the reciprocal number of the exponential factor, n, of the ΔP-Q equation for the envelope takes on 2.

The airtightness levels (abscissas of the graphs) are for 9.8 Pa (1 mmAq) of the reference pressure difference. The graphs for air change rate vs. airtightness are linear in the range of $SLA_{9.8}$ up to 3 cm^2/m^2. But when $SLA_{9.8}$ becomes greater, the air change rate does not show a linear increase because of the greater influence of the airflow resistance through the undercuts (160 mm in diameter). When compared at a fixed airtightness level, the air change rate becomes greater approximately in proportion to $\Delta\theta^{0.54}$ to $\Delta\theta^{0.55}$ ($\Delta\theta$ for internal-external temperature difference in K).

Even if the effective leakage area is constant, the air change rate necessarily changes, depending upon the reciprocal number of the exponential factor of ΔP or a reference pres-

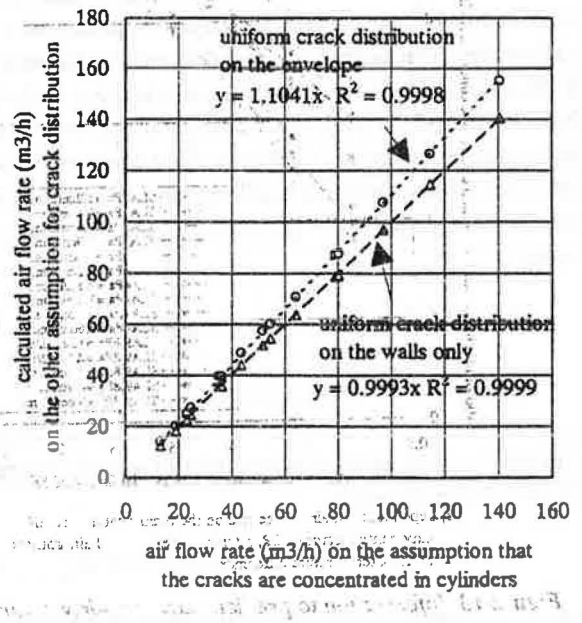

***Figure 12** Comparison between airflow rates on the different assumptions for crack distribution.*

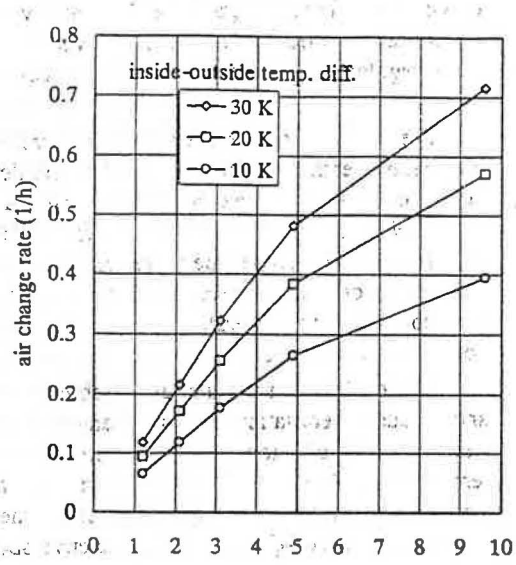

(a) Air Change Rate Plotted against Specific Leakage Area at the Reference Pressure 1 mmAq (9.8 Pa). The Reciprocal Number of Exponential of ΔP in Q-ΔP Equation is 2

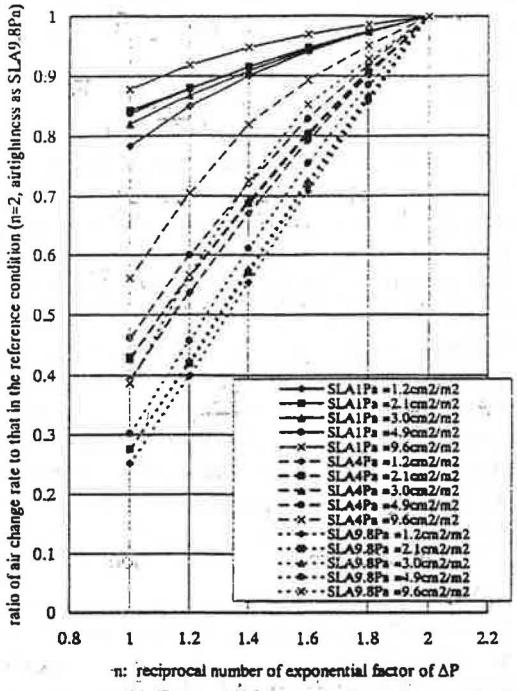

(b) dependence of air change rate on the reciprocal number of exponential factor of ΔP, reference pressure and airtightness at 10 deg.K temperature difference

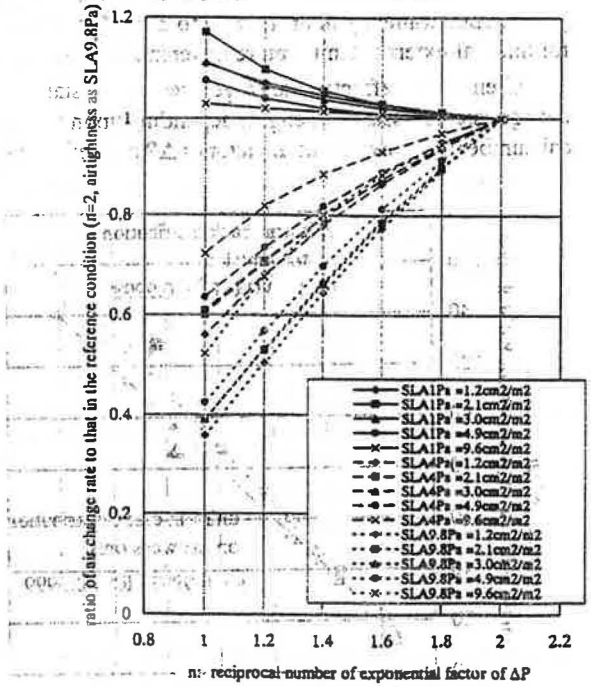

(c) dependence of air change rate on the reciprocal number of exponential factor of ΔP, reference pressure and airtightness at 20 K temperature difference

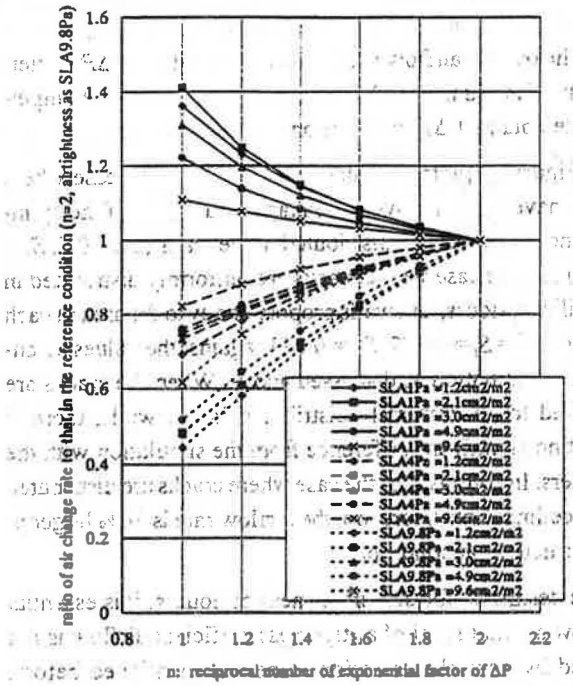

(d) dependence of air change rate on the reciprocal number of exponential factor of ΔP, reference pressure and airtightness at 30 K temperature difference

Figure 13 Information to predict buoyancy-driven air change rate in a two-story house with an envelope of different leakage characteristics.

sure difference. The air change rates for different exponents and reference pressure differences were calculated, and the ratios of the values obtained to those in the reference condition ($n = 2$, $\Delta P_{ref} = 9.8$ Pa [1 mmAq]) are indicated in Figure 13(b), (c), and (d).

When $n = 2$, the effective leakage area is constant regardless of the reference pressure; therefore, the air change rate is not influenced by reference pressure. At an internal-external temperature difference of 10 K (Figure 13b), the influence of the value of n on the air change rate is smallest when the reference pressure difference is 1 Pa and is largest for 9.8 Pa (1 mmAq). When the specific leakage area at a reference pressure difference of 4 Pa is 1.2 cm^2/m^2, the air change rate with $n = 1.6$ is 20% smaller than with $n = 2$. At an internal-external temperature difference of 20 K (Figure 13c) also, the dependency on the value of n is smaller when the reference pressure difference is 1 Pa. This can be explained by the fact that the pressure differences across the envelope when airflow is due to buoyancy are 0.5 to 1.5 Pa, i.e., around 1 Pa, as shown in Figure 10c.

The air change rate varies more significantly, depending upon the value of n, if 4 Pa or 9.8 Pa is selected for the reference pressure difference at internal-external temperature differences of 10 K or 20 K. When the temperature difference is 30 K, there is no obvious difference in dependency of the air change rate on the value of n whether 1 Pa or 4 Pa is selected for the reference pressure difference. Through comparison of (b), (c), and (d) in Figure 13, the influence of the value of n on the air change rate is not independent of the internal-external temperature difference.

Using the airflow rate (air change rate) as a reference value, with $n = 2$ and reference pressure difference = 9.8 Pa, determined from Figure 13(a) by airtightness and internal-external temperature difference, the air change rates along with other exponents and reference pressures can be obtained by multiplying the reference value by the coefficients given by Figure 13(b),13(c), and 13(d). For example, if the temperature difference is 10 K, the reference pressure difference is 1 Pa, n is 1.6, and the air change rate is calculated by multiplying the rate given by Figure 13(a) by a factor of 0.95, regardless of airtightness. When the temperature difference is 30 K and n is 1.2, the buoyancy-driven air change rate can be predicted, if $SLA_{9.8}$ is within the range from 1 to 5, by multiplying by a factor of 0.6 the air change rate determined by Figure 13(a).

CONCLUSIONS

1. A full-scale experimental house (cylinder house) was constructed in an artificial climate chamber, where cylinders were installed for simulating airflow paths, including cracks in the envelope and internal walls, and the flow rate through the cylinders were determined by measuring the pressure difference across them. With these facilities, it was confirmed that the airflow pattern can be measured without using tracer gas. The measurement result is applicable to the validation of tracer gas measurement techniques and network simulation programs.
2. Through a series of tests with the cylinder house, the variation of airflow rate due to buoyancy, depending on door status (open or closed) inside the house and undercut size, was observed. The experimental results demonstrate that, in houses with a leaky envelope, the status of doors exerts significant influence on the buoyancy-driven airflow rate.
3. Satisfactory agreement was confirmed between values obtained by basic calculation and measured data for the buoyancy-driven airflow rates and pressure differences across the envelope. Then, using the same calculation technique, it was verified that the airflow induced by buoyancy when cracks are uniformly distributed in the walls is almost the same as that when cracks are concentrated at several positions (cylinders) in the walls.
4. Employing the calculation method verified by experimental data, the air change rates were plotted against the airtightness of the envelope ($SLA_{9.8}$), at internal-external temperature differences of 10 K, 20 K, and 30 K, fixing the room temperature at 20°C. Calculation was also done with reciprocal numbers of the exponential factor of ΔP other than 2 and with reference pressure differences other than 9.8 Pa (1 mmAq) for determining the airtightness, and the ratios of the calculated results to the values in the reference condition ($n = 2$, $\Delta P_{ref} = 9.8$ Pa [1 mmAq]) were plotted. These graphs will enable prediction of the air change rate due to buoyancy with different exponents and reference pressure differences.
5. Ventilation design in airtight houses is an important subject. If, at a given airtightness of the envelope and an internal-external temperature difference, the buoyancy-induced airflow rate is determined in order to predict the natural airflow rate, the resultant estimation is conservative in terms of maintaining good air quality. Such prediction enables us to know the critical airtightness of the envelope that requires mechanical ventilation for ensuring the required air change rate. Also, when a natural ventilation system is selected on the basis of the predicted critical airtightness, it is possible to provide the required number of natural vents considering the effective leakage area of each vent. It is also possible to use natural vents designed with a flow-controlling mechanism to prevent degradation of thermal comfort and heat loss due to excessive airflow.

REFERENCES

Afonso, C.F.A., E.A.B. Maldonado, and E. Skåret. 1986. A single tracer-gas method to characterize multi-room air exchanges. *Energy and Buildings* 9.

ASHRAE. 1989. *1989 ASHRAE handbook—Fundamentals*, p. 23.17. Atlanta: American Society of Heating, Refrigerating and Air-Conditioning Engineers, Inc.

Enai, M., C.Y. Shaw, J.T. Reardon, and R.J. Magee. 1990. Multiple tracer gas techniques for measuring interzonal

airflows for three interconnected spaces. *ASHRAE Transactions* 96(1).

IEA. 1996. *IEA Annex 27, Evaluation and demonstration of domestic ventilation systems, Subtask 1 Report*. Air Infiltration and Ventilation Center.

Okuyama, H. 1990. System identification theory of the thermal network model and application for the multi-chamber airflow measurement. *Building and Environment* 25.

Shaw, C.Y. 1987. Methods for estimating air change rates and sizing mechanical ventilation systems for houses. *ASHRAE Transactions* 93(2): 2284-2302.

Sherman, M.H., and D.T. Grimsrud. 1980. Infiltration-pressurization correlation: Simplified physical modeling. *ASHRAE Transactions* 86(2): 778-807.

Sinden, F.W. 1978. Multi-chamber theory of air infiltration. *Building and Environment* 13.